# QUASAR-LYMAN $\alpha$ FOREST CROSS-CORRELATION FROM SDSS-III BOSS SURVEY: BARYON ACOUSTIC OSCILLATIONS

Hélion du MAS des BOURBOUX
*CEA-Saclay, Irfu F-91191 Gif-sur-Yvette, France*

We measure the large-scale cross-correlation of quasars with the Lyman-$\alpha$ forest absorption field. We use over 170,000 forests from Data Release 12 (DR12) of the SDSS-III BOSS survey and over 240,000 quasars from DR12 and from DR7 of the SDSS-II survey. This study allows us to measure the Baryonic Acoustic Oscillation (BAO) scale, along and across the line-of-sight, at a mean redshift of z = 2.40. These scales are linked to the Hubble parameter and the angular diameter distance, respectively. We produced a set of 100 Gaussian random field simulations. The covariance of the set is found to agree with the covariance matrix calculated from the data. These simulations will be used in the future to search for a possible bias in the measurement of the BAO scale.

## 1 Introduction

During the last decade the Baryonic Acoustic Oscillation (BAO) scale has proved itself a very powerful measure of the expansion of the Universe related to the dark matter and dark energy redshift evolution. The Lyman-$\alpha$ auto-correlation [1] and Lyman-$\alpha$-quasar cross-correlation [2] measure the BAO parameters: $\alpha_{\parallel} = D_H(z)/r_d(z_d)$ and $\alpha_{\perp} = D_A(z)/r_d(z_d)$ at a mean redshift of $z = 2.40$, with $r_d$ the sound horizon.

The Lyman-$\alpha$ (Ly$\alpha$) forest is the pattern seen in a quasar spectrum between the Ly$\beta$ emission line ($\lambda_{R.F.} = 1025.72$ Å) and the Ly$\alpha$ emission line ($\lambda_{R.F.} = 1215.67$ Å). This absorption is mainly induced by the presence of neutral hydrogen in the intergalactic medium. A small fraction of the absorption is also linked to the presence of metals: mainly carbon, magnesium, silicon and iron. A Ly$\alpha$ density fluctuation $\delta_\alpha$ is related to a dark matter density fluctuation $\delta_{DM}$ by the bias parameter $b_\alpha$:

$$\delta_\alpha = b_\alpha \cdot \delta_{DM}. \tag{1}$$

In a similar way, quasars (QSO) traces matter fluctuations with a bias $b_{QSO}$. The matter clustering can then be estimated with the cross-correlation between Ly$\alpha$ forest pixels and quasars:

$$\xi^{qf}(\vec{r}) = < \delta_\alpha(\vec{x}) \cdot \delta_q(\vec{x} + \vec{r}) > . \tag{2}$$

A measurement of this function was done by Font-Ribera et al.[2] using the Data Release 11 (DR11) of the SDSS-III Baryon Oscillation Spectroscopic Survey (BOSS). The study measured $\alpha_{\parallel} = 1.042 \pm 0.034$ and $\alpha_{\perp} = 0.930 \pm 0.036$.
The improvements of this new study are: an increase of statistics with the final quasar catalogue DR12 of BOSS, improvements in the data reduction, and the development of Gaussian random field simulations. These simulations will allow us to validate the measured parameters.

## 2 BOSS quasar sample and data reduction

The BOSS observations ran from 2009 to 2014 and covered $10^4$ deg$^2$ on the sky. We use over 170,000 forests from DR12 of the SDSS-III BOSS survey and over 240,000 quasars from DR12 and from DR7 of the SDSS-II survey. The Ly$\alpha$ forest is defined for rest frame wavelength $\lambda_{R.F.} \in [1040, 1200]$ Å and for observed wavelength $\lambda_{Obs.} \in [3600, 7235]$ Å. Assuming Ly$\alpha$ to be the main absorber, we cover the redshift range $z \in [1.96, 4.95]$.

A Ly$\alpha$ absorption fluctuation is defined by:

$$\delta_{\alpha}^{l,i} = \frac{f^{l,i}}{\overline{F}(\lambda_{Obs.}^{l,i}) \cdot \overline{C}(\lambda_{R.F.}^{l,i}) \cdot (a^l + b^l \lambda_{R.F.}^{l,i})} - 1, \tag{3}$$

where $l$ is for a given quasar forest and $i$ is for a pixel of this forest, $f^{l,i}$ is the observed flux. $\overline{C}$ is the unabsorbed quasar continuum. It is allowed to vary linearly from forest to forest, with parameters $a^l$ and $b^l$. Finally, $\overline{F}$ is the mean transmitted flux fraction, giving the evolution of neutral hydrogen density. For the data, Figure 1 shows, in blue, the quasar continuum on the left panel and the mean transmitted flux fraction on the right panel.

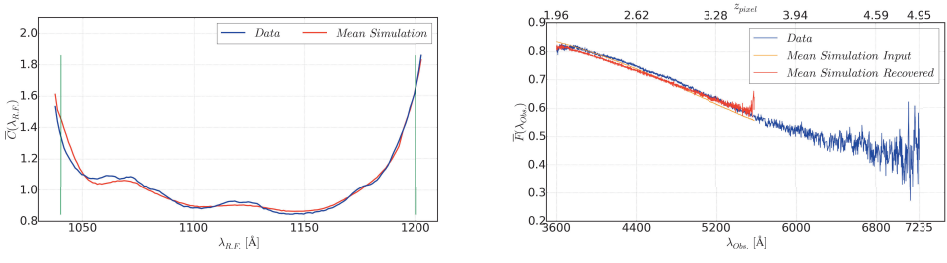


Figure 1 – Left pannel: unabsorbed quasar continuum for data in blue and for simulations in red in the rest frame wavelength range of the Ly$\alpha$ forest. Right pannel: mean transmitted flux fraction for data in blue, for simulations in red and for simulation input in orange.

The quasar catalogue provides us with a boolean information of the matter density field. The Ly$\alpha$-quasar cross-correlation is then defined by:

$$\xi^{qf}(\vec{s}) = \frac{\sum\limits_{(i,k)\ at\ \vec{s}} w_{\alpha}^{i}\, \delta_{\alpha}^{i}}{\sum\limits_{(i,k)\ at\ \vec{s}} w_{\alpha}^{i}}, \tag{4}$$

where $i$ is a forest pixel, $w_{\alpha}^{i}$ is the pixel weight, $k$ is a quasar and $\vec{s}$ is the comoving redshift space vector between the pixel and the quasar.

Figure 2 shows, in blue, the Ly$\alpha$-QSO cross-correlation for data as a function of the comoving redshift space separation. The cross-correlation is rescaled by a factor $|s|^2$ in order to see the BAO scale. This scale appears as a dip in the correlation function around $r_s \approx 105$ h$^{-1}$Mpc. When a Ly$\alpha$ pixel is close to a QSO, it sits in a higher density region and thus absorbs more flux. This explains why the correlation function is negative at small scales. Data error bars are

calculated using 80 sub-samples. In this method, the data set is separated in 80 regions acording to the forests position on the sky. The cross-correlation is calculated in each sub-divisions of the sky. The errors are then given by the covariance of the set.

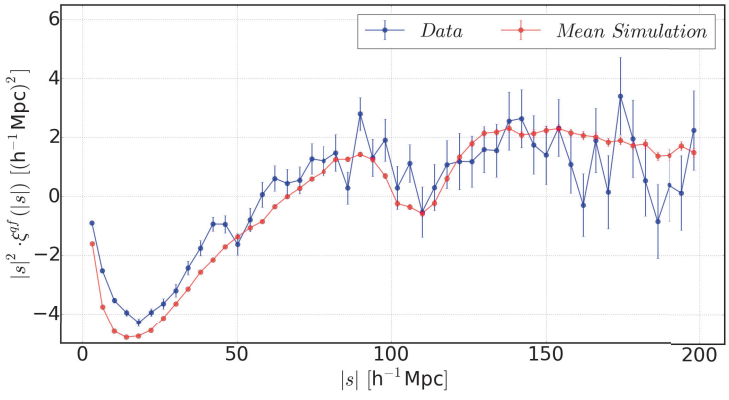


Figure 2 – Ly$\alpha$-quasar cross-correlation monopole as a function of comoving redshift space coordinate. The monopole is multiplied by a factor $|s|^2$. In blue the data with sub-sampling errors. In red the mean over the 100 simulations with errors given by the variance of the set.

## 3 Simulation and data comparison

### *3.1 Description*

We have developed simulations of the cross-correlation measurement. They allow us to test our covariance matrix estimation, to look for possible biases in our data extraction process. These simulations have been performed following J.-M. Le Goff et al. [3]. We use the fiducial cosmology of a flat ΛCDM Universe ($h = 0.7$, $\Omega_b h^2 = 0.0227$, $\Omega_c h^2 = 0.1096$, $\sigma_8 = 0.794961$). The linear matter power spectrum is calculated with CAMB. A Gaussian random field is generated over a comoving volume of 11 Gpc$^3$ with this power spectrum. Pixels have a comoving size $a_{LR} = 3.15$ h$^{-1}$Mpc. The box center has a redshift of $z = 2.50$.

Quasars are defined to sit in pixels where overdensities are greater than $\delta_{cut}$. In order to have a similar bias as the data, we set this threshold using Padmanabhan and White [4] to get $b_{QSO} = 3.6$ at $z = 2.50$. A random selection of these pixels are rejected in order to reproduce the redshift distribution of quasars in data and their number density. The QSO position is randomly selected within the volume of the pixel. Their redshift is shifted according to the line-of-sight velocity of the pixel.

Forests are drawn along the line-of-sight of these quasars. High resolution boxes of comoving edge length $l_{HR} = 3.15$ h$^{-1}$Mpc and pixels comoving size $a_{HR} = l_{HR}/16 \approx 0.2$ h$^{-1}$Mpc are placed in the low resolution box pixels. This process allows us to reproduce the level of noise in the data along with the 1D forest correlation $\xi^{1D,ff}$: the correlation between pixels along the line-of-sight of a quasar. The density fluctuation and the velocity of a pixel is then translated to a transmission field using the Gunn-Peterson approximation:

$$F = \exp[-a(z) f(v) \exp(\gamma g(z)(\delta_{LR} + \delta_{HR}))], \tag{5}$$

where $f$ is a function of the velocity of neighbouring pixels and $g$ is the linear growth factor. The function $a$ and the parameter $\gamma$ are set to reproduce the mean transmitted flux fraction and

the bias evolution of data. In the right panel of Figure 1, the orange curve shows the evolution of $\overline{F}$ in the simulation as a function of observed wavelength. We can see that it is very similar to the evolution of $\overline{F}$ in the data, in blue on the same graph.

The mock expander, described in J. E. Bautista et al. [5], transforms the transmission $\overline{F}$ in flux $\phi$. It adds the resolution of the SDSS-III BOSS spectrograph, the continuum and magnitude properties of the BOSS quasars and the level of noise of the data.
We also add absorbtions of the relevant metals for the cross-correlation: Si-II (1190 Å), Si-II (1193 Å), Si-II (1260 Å) and Si-III (1207 Å). Parameters of the metal absorbtion field are set in order to reproduce the $\xi^{1D,ff}$ measured in data. These are the only relevant transitions for the cross-correlation. Other transitions only induce noise in our measurement.

As a result, we get a set of 100 full simulations, reproducing the most important properties of the data. These are the first simulations with simultaneously three correlations: forests auto-correlation $\xi^{ff}$, quasar-forest cross-correlation $\xi^{qf}$ and quasar auto-correlation $\xi^{qq}$. The 1D correlation $\xi^{1D,ff}$ is also reproduced.

In Figure 2, we show, in red, the stack of the 100 simulated cross-correlation monopoles. The error bars are computed from the variance of the set. The BAO scale is the dip at $r_s \approx 105$ h$^{-1}$Mpc. The differences between the data and the simulations at small scales ( $|s| < 50$ h$^{-1}$Mpc) are caused by two effects: a small difference of biases between the data and the simulations, and other aspects. This is expected to have no effect on the values of the BAO parameters, because biases have no correlations with them.

In practice we fit the cross-correlation $\xi(\vec{s}) = \xi(s_\perp, s_\parallel)$. In Figure 3 we show the covariance matrix normalized to its diagonal (i.e. the correlation matrix). On both plot, the matrix is estimated using sub-samples on data in blue and using simulations in red. The left plot shows the mean of the correlation matrix for bins with same $s_\perp$. The right plot shows the correlation matrix for bins with $|\Delta s_\perp| = 4$ h$^{-1}$Mpc. We can see that the matrix is nearly diagonal. Sub-samples and simulations give similar results.

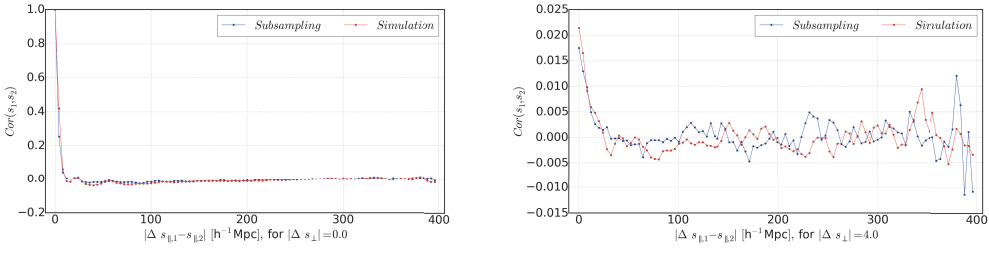


Figure 3 – Correlation matrix of the Ly$\alpha$-quasar cross-correlation. Left pannel: mean correlation between two bins $\vec{s_1}$ and $\vec{s_2}$ when $|\Delta s_\perp| = 0$ h$^{-1}$Mpc. Right pannel: mean correlation between two bins when $|\Delta s_\perp| = 4$ h$^{-1}$Mpc.

## References


1. T. Delubac et al. Baryon acoustic oscillations in the Ly$\alpha$ forest of BOSS DR11 quasars. Astronomy and Astrophysics, 574:A59, February 2015.
2. A. Font-Ribera et al. Quasar-Lyman $\alpha$ forest cross-correlation from BOSS DR11: Baryon Acoustic Oscillations. Journal of Cosmology and Astroparticle Physics, 5:027, May 2014.
3. J. M. Le Goff et al. Simulations of BAO reconstruction with a quasar Ly-$\alpha$ survey. Astronomy and Astrophysics, 534:A135, October 2011.
4. N. Padmanabhan and M. White. Calibrating the baryon oscillation ruler for matter and halos. Phys. Rev. *D*, 80(6):063508, September 2009.
5. J. E. Bautista et al. Mock Quasar-Lyman-$\alpha$ forest data-sets for the SDSS-III Baryon Oscillation Spectroscopic Survey. Journal of Cosmology and Astroparticle Physics, 5:060, May 2015.